Crystal habit modification of metronidazole by supramolecular gels with complementary functionality

Sreejith Sudhakaran Jayabhavan,[†] Jonathan W Steed,*[‡] and Krishna K. Damodaran*[†]

[†]Department of Chemistry, Science Institute, University of Iceland, Dunhagi 3, 107 Reykjavík, Iceland. Tel: +354 525 4846, Fax: +354 552 8911.

[‡]Department of Chemistry, Durham University, South Road, Durham DH1 3LE, UK

ABSTRACT: A series of bis(urea) compounds with complementary functional groups similar to pharmaceutical drug metronidazole, and a structural isomer isometronidazole have been synthesized. The gelation properties of these compounds were studied in various solvent/solvent mixtures. The mechanical strength of the isomeric gelators was compared using rheology and the morphologies of the xerogels were analyzed by scanning electron microscopy. These gels were used as media for metronidazole crystallization resulting in marked habit modification of the metronidazole crystals in the drug mimicking gels. However, crystallization in the non-mimetic isomeric gel resulted in similar morphologies to the solution state. These results indicate that the drug-mimetic gels interact with the surface of the drug crystal giving rise to new morphologies.

INTRODUCTION

Supramolecular gels based on low molecular weight gelators (LMWGs)[1-7] have become highly topical in the last two decades owing to their intriguing potential applications in drug delivery, separation techniques, as templates for inorganic and polymer materials and as media for crystallization. Crystallization in gel media dates back at least as far as the discovery of the well-known 'Liesegang rings,' which represent periodic precipitation in gels.[8] Gel phase crystallization represents an example of orthogonal self-assembly of the crystals and gel network.[9] The gel medium limits convection and prevents sedimentation by providing continuous, diffusion-limited growth,[10, 11] as well as influencing the nucleation behavior of the crystals.[12] LMWGs have been used to crystallize inorganic substances, proteins, and active pharmaceutical ingredients,[13-18] and the gel environment can influence factors such as crystal habit and polymorphism.[9] LMWGs can provide various advantages as media for crystal growth, such as facile synthesis, long shelf-life, and easy modification of functional groups. There have been a few recent reports of crystallization within LMWG;[9] for example, calcite crystallization in a bis(urea) gel[19] and crystallization of aspirin, caffeine, indomethacin and carbamazepine in toluene-based tetraamide organogels.[20] We have shown that LMWGs can be used as a medium for crystallizing inorganic complexes and reported the selective crystallization of one particular form (form-I) of a copper(II) isonicotinate–*N*-oxide complex.[21] We have shown that designing gelators that mimic the crystallization substrate can enable the gelator molecules to interact with the substrate, offering the possibility of epitaxial crystal growth and hence favoring metastable or hard-to-nucleate solid forms of molecular crystals including pharmaceutically relevant compounds.[9-11, 19-27]

Previous work on gel phase crystallization using crystallization substrate mimicking gelators has resulted in crystal habit modification of isoniazid[28] and cisplatin.[29] Crystallization in bis(urea) LMWGs tagged with functional groups (Scheme 1) similar to a highly polymorphic drug precursor, ROY, resulted

in the selective crystallization of the metastable R polymorph in contrast to the Y form obtained in solution.[10] Recently, drug mimicking LMWGs have been used to prevent concomitant crystallization.[30] Thus, structural similarity between the crystallization substrate and the gelator is potentially significant in gel phase crystallization. In the present work, we have designed bis(urea) compounds that mimic the antibiotic metronidazole as well as isomeric control gelators in order to study the outcome of the drug-mimetic gel phase crystallization of this drug substance.
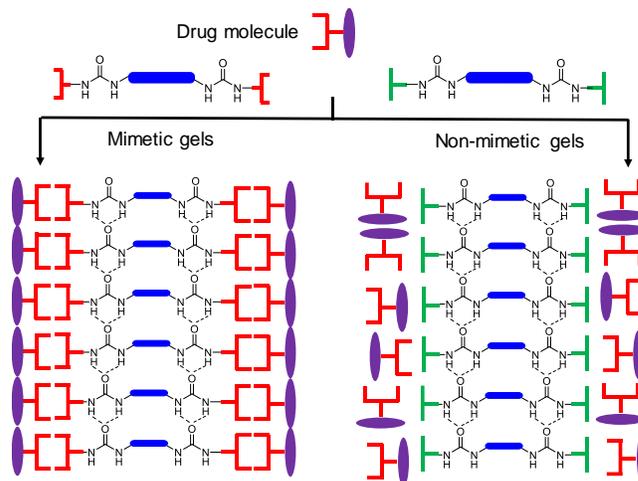
Scheme 1: Gel phase crystallization in drug-mimetic and non-mimetic gels, red line represents drug mimicking functional groups and green line indicates random functional groups. Specific interactions between gel fiber and drug in the mimetic case can give rise to changes in morphology and polymorphic form.

Metronidazole, a nitroimidazole antibiotic, is used to treat periodontal disease and shows activity against anaerobic protozoa and bacteria.[31-34] There are two polymorphs reported for this drug in the Cambridge Structural Database[35] (form-I, CSD refcode MNIMET)[36] and (form II, CSD refcode MNIMET01). The

solid forms of metronidazole are an area of interest as a result of its poor tableting properties. Martino *et al.* have demonstrated that the crystal habit of metronidazole is influenced by both the solvent polarity index and the crystallization method.[37] This prompted us to study gel phase crystallization of metronidazole using drug mimicking compounds as gelators. However, designing LMWGs with specified properties and structure is challenging and LMWGs are often discovered by serendipity. This is due to the fact that the structure and properties of the supramolecular gels rely primarily on the geometry and spatial arrangement of the building blocks and also the nature of intermolecular interactions.[38, 39] The gel–solute interactions can potentially affect both nucleation and crystal growth rates in a supramolecular gel phase crystallization.[40] Thus, the spatial arrangement of the functional groups and gelator aggregation mode are both of interest in supramolecular gel phase crystallization. We have designed gelators based on bis(urea) backbone with a complementary functional group similar to metronidazole and isometronidazole. The urea motif chosen is well known to form α-tapes resulting in fibrils that could align the drug-derived functional groups as a locally ordered array on the surface of the gel fibers (Scheme 1).[3, 41, 42] The resulting LMWGs are anticipated to have a fibrous surface that chemically matches the crystallization substrate,[10] which offers the possibility of epitaxial crystal growth.[9] We have selected structural isomers as the complementary functional groups to analyze study the effect of positional isomers on gelation in LMWGs. In this work we report the gelation and gel phase crystallization in LMWGs based on derivatives of both metronidazole and its structural isomer isometronidazole. Comparison of the gelation abilities of metronidazole and isometronidazole bis(urea) compounds will enable us to study the role of the position of functional groups on gelation and gel phase crystallization in LMWGs.

EXPERIMENTAL SECTION

Materials and methods

All the starting materials and reagents were commercially available (Sigma Aldrich and TCI Europe) and used as supplied except metronidazole, which was purchased from Accel Pharmtech, USA. ^{1}H and ^{13}C NMR spectra (Figure S1-12, see supporting information) were recorded on a Bruker AVANCE 400 spectrometer and SEM was performed on a Leo Supra 25 microscope. SCXRD and powder X-ray diffraction (PXRD) was carried out using Bruker D8 venture and PANalytical instrument.

Synthesis

The bis(urea) compounds of metronidazole (**1-3**) and isometronidazole (**4-6**) were synthesized following a general procedure by reacting the amine precursors with the corresponding diisocyanates. The amine precursors of metronidazole and isometronidazole were synthesized as described below.

1. Synthesis of 1-(2-bromoethyl)-2-methyl-5-nitro-1H-imidazole (**7**): Compound **7** was synthesized by slightly modifying the reported procedure.[43] Bromine solution (1.6 mL, 32.2 mmol) was added to a stirred solution of triphenylphosphine (8.4 g, 32.1 mmol) in DCM (100 mL) at 0 °C , followed by the dropwise addition of triethylamine (4.5 mL, 32.0 mmol). Metronidazole (5.0 g, 29.2 mmol) was added in portion to the above solution and was equilibrated to room temperature after 10 minutes. The mixture was stirred for 30 minutes, and the excess

bromine was quenched with a saturated solution of aqueous sodium thiosulphate (10.0 mL). Water (50.0 mL) was added to the mixture and the organic phase was separated and treated with 40.0 mL of 1.0 ~~N~~ MHCl. The organic phase was discarded, and the aqueous layer was extracted with DCM (3 x 30 mL) to remove the excess triphenylphosphine oxide impurities. The solution was treated with 2.0 ~~N~~ Msodium hydroxide solution to precipitate the product, which was extracted with DCM (3 x 40 mL), dried over sodium sulfate and evaporated in a rotary vapor to yield the product as a yellow solid. Yield: 78.0 %. ^{1}H NMR (400 MHz, chloroform-*d*) δ 7.97 (s, 1H), 4.67 (t, *J* = 6.2 Hz, 2H), 3.69 (t, *J* = 6.2 Hz, 2H), 2.57 (s, 3H). ^{13}C{^{1}H} NMR (100 MHz, chloroform-*d*) δ 151.12, 138.24, 133.51, 47.40, 29.53, 14.81. HRMS (APCI): calcd for $C_6H_9N_3O_2BrN$ [M + H]⁺, 233.9873; found, 233.9862.

2. Synthesis of 1-(2-azidoethyl)-2-methyl-5-nitro-1H-imidazole[43] (**8**): Sodium azide (1.25 g, 19.8 mmol) was added in portions to a solution of compound **7** (3.0 g, 12.8 mmol) in 40.0 mL DMF and the mixture was stirred at 60 °C for 22 h. The solvent DMF was evaporated, and 40 mL water was added. The mixture was extracted with DCM (3 x 40 mL) and the organic parts were combined, dried over sodium sulfate, and evaporated to get the product as a yellowish powder. Yield: 99.0 %. ^{1}H NMR (400 MHz, chloroform-*d*) δ 7.98 (s, 1H), 4.44 (dd, *J* = 6.0, 5.0 Hz, 2H), 3.78 (t, *J* = 6.1 Hz, 2H), 2.54 (s, 3H). ^{13}C{^{1}H} NMR (100 MHz, chloroform-*d*) δ 151.33, 138.29, 133.42, 50.98, 45.57, 14.57. HRMS (APCI): calcd. for $C_6H_9N_6O_2$ [M + H]⁺, 197.0781; found, 197.0776.

3. Synthesis of 2-(2-methyl-5-nitro-1H-imidazol-1-yl)ethan-1-amine[44] (**9**): Compound **8** (5.8 g, 29.6 mmol) was dissolved in a mixture of 60.0 mL of THF and 7.5 mL water and was treated with triphenylphosphine (16.3 g, 62.2 mmol). The mixture was stirred at room temperature for 15 h and was concentrated (~10.0 mL). The mixture was treated with 2.0 ~~N~~ M HCl (20.0 mL) and was washed with DCM (3 x 30 mL) to remove the impurities. The aqueous layer was evaporated to obtain a white powder, which was washed with methanol/DCM mixture (1:9, v/v) to yield amine dihydrochloride (**9**.2HCl). The crude product was recrystallized from acidic DMF solution. Yield: 73.0 %. ^{1}H NMR (400 MHz, DMSO-*d₆*) δ 8.57 (s, 3H), 8.37 (s, 1H), 4.62 (t, *J* = 6.6 Hz, 2H), 3.30 – 3.17 (m, 2H), 2.61 (s, 3H). ^{13}C{^{1}H} NMR (100 MHz, DMSO-*d₆*) δ 150.43, 137.79, 129.16, 42.98, 37.28, 12.93. HRMS (APCI): calcd for $C_6H_{10}N_4O_2Na$ [M + H]⁺, 171.0877; found, 171.0876.

4. Synthesis of 1-(2-bromoethyl)-2-methyl-4-nitro-1H-imidazole[45] (**10**): A solution of 2-methyl-4-nitro-1H-imidazole (5.0 g, 39.3 mmol), potassium carbonate (13.5 g, 97.6 mmol), 1,2-dibromoethane (17.0 mL, 196.5 mmol) was prepared in 50.0 mL DMF and the mixture was stirred overnight at room temperature. The solution was evaporated, and 40.0 mL of water was added and extracted with DCM (3 x 30 mL). The organic layers were combined and evaporated to dryness. The crude product was obtained as a yellow-white solid, which was purified by column chromatography (eluent: DCM with methanol gradient, 0 - 0.5%). Yield: 65.0 %. ^{1}H NMR (chloroform-*d*, 400 MHz) δ 7.77 (s, 1H), 4.36 (t, *J* = 6.1 Hz, 2H, 3.64 (t, *J* = 6.1 Hz, 2H), 2.47 (s, 3H). ^{13}C{^{1}H} NMR (100 MHz, chloroform-*d*) δ 146.83, 144.97, 119.62, 48.32, 29.21, 13.33. HRMS (APCI): calcd for $C_6H_8N_3O_2BrNa$ [M + Na]⁺, 255.9692; found, 255.9693.

5. Synthesis of 1-(2-azidoethyl)-2-methyl-4-nitro-1H-imidazole (**11**): The reaction procedure was similar to compound **8**. Compound **10** (3.2 g, 13.7 mmol), sodium azide (1.3 g, 20.5 mmol)

and 40.0 mL DMF. Yield: 98.0 %. ^{1}H NMR (400 MHz, chloroform-d) δ 7.76 (s, 1H), 4.08 (t, J = 6.1 Hz, 2H), 3.73 (t, J = 6.1 Hz, 2H), 2.45 (s, 3H). ^{13}C{^{1}H} NMR (100 MHz, chloroform-d) δ 146.75, 145.04, 119.80, 50.86, 46.12, 13.16. HRMS (APCI): calcd for $C_6H_8N_6O_2Na$ [M + Na]$^+$, 219.0601; found, 219.0598.

6. Synthesis of 2-(2-methyl-4-nitro-1H-imidazol-1-yl)ethan-1-amine[44] (**12**): The reaction procedure was similar to compound **9.** Compound **11** (2.25 g, 11.5 mmol), triphenylphosphine (6.17 g, 23.6 mmol) and THF/water (20/2.5 mL). The amine was re-crystallized as a hydrochloride salt in acidic ethanol solution (**12**.HCl). Yield: 73.0 %. ^{1}H NMR (400 MHz, DMSO-d_6) δ 8.43 (s, 1H), 8.37 (s, 3H), 4.32 (t, J = 6.1 Hz, 2H), 3.25 (t, J = 6.1 Hz, 2H), 2.40 (s, 3H). ^{13}C{^{1}H} NMR (100 MHz, DMSO-d_6) δ 145.59, 145.50, 122.36, 43.69, 38.28, 12.76. HRMS (APCI): calcd for $C_6H_{10}N_4O_2Na$ [M + Na]$^+$, 193.0696; found, 193.0692.

7. Synthesis of bis(3,5-diethyl-4-isocyanatophenyl)methane (**13**): The bis(isocyanate) was synthesized according to a reported procedure.[46] Yield: 95.0 %. ^{1}H NMR (400 MHz, chloroform-d) δ 6.87 (s, 4H), 3.85 (s, 2H), 2.65 (q, J = 7.6 Hz, 8H), 1.22 (t, J = 7.6 Hz, 12H). ^{13}C{^{1}H} NMR (100 MHz, chloroform-d) δ 138.91, 138.49, 127.96, 126.94, 41.12, 25.70, 14.24.

General procedure for the synthesis of bis(urea) compounds: The amine hydrochloride (2.1 equiv) was dissolved in chloroform by adding triethylamine (4.0 equiv) at room temperature. A solution of the corresponding diisocyanate (1.0 equiv) was added dropwise to the above mixture and was refluxed overnight under a nitrogen atmosphere. The precipitate formed was filtered and stirred with saturated sodium bicarbonate solution for 24 h. The mixture was filtered, the residue was washed with a copious amount of water and dried to isolate the product.

8. Synthesis of 1,1'-(hexane-1,6-diyl)bis(3-(2-(2-methyl-5-nitro-1H-imidazol-1-yl)ethyl)urea) (**1**): The crude compound was re-crystallized from ethanol. Yield: 75.0 %. ^{1}H NMR (400 MHz, DMSO-d_6) δ 8.00 (s, 2H), 6.01 – 5.90 (m, 4H), 4.29 (t, J = 5.7 Hz, 4H), 3.37 – 3.28 (m, 4H), 2.90 (q, J = 6.4 Hz, 4H), 2.38 (s, 6H), 1.29 (m, 4H), 1.24 – 1.15 (m, 4H). ^{13}C{^{1}H} NMR (100 MHz, DMSO-d_6) δ 157.23, 150.88, 137.82, 132.50, 45.73, 38.55, 38.21, 29.31, 25.46, 13.12. HRMS (APCI): calcd for $C_{20}H_{32}N_{10}O_6Na$ [M + Na]$^+$, 531.2398; found, 531.2403.

9. Synthesis of 1,1'-(1,3-phenylenebis(propane-2,2-diyl))bis(3-(2-(2-methyl-5-nitro-1H-imidazol-1-yl)ethyl)urea) (**2**): The crude material was recrystallized from iso-propanol. Yield: 72.0 %. ^{1}H NMR (400 MHz, DMSO-d_6) δ 8.00 (s, 2H), 7.27 (s, 1H), 7.24-7.14 (m, 1H), 7.08 (d, J = 7.7 Hz, 2H), 6.28 (s, 2H), 5.91 (t, J = 6.0 Hz, 2H), 4.27 (t, J = 5.4 Hz, 4H), 3.37-3.28 (m, 4H), 2.41 (s, 6H), 1.47 (s, 12H). ^{13}C{^{1}H} NMR (100 MHz, DMSO-d_6) δ 156.22, 150.91, 147.51, 137.84, 132.52, 126.69, 121.80, 120.63, 53.65, 45.84, 37.84, 29.26, 13.25. HRMS (APCI): calcd for $C_{26}H_{36}N_{10}O_6Na$ [M + Na]$^+$; found, 607.2712.

10. Synthesis of 1,1'-(methylenebis(2,6-diethyl-4,1-phenylene))bis(3-(2-(2-methyl-5-nitro-1H-imidazol-1-yl)ethyl)urea) (**3**): The crude compound was re-crystallized in ethanol. Yield: 75.0 %. ^{1}H NMR (400 MHz, DMSO-d_6) δ 7.98 (s, 2H), 7.39 (s, 2H), 6.91 (s, 4H), 6.26 (s, 2H), 4.32 (t, J = 5.7 Hz, 4H), 3.78 (s, 2H), 3.45 (s, 4H), 2.44 (s, 6H), 2.39-2.32 (m, 8H), 1.03 (t, J = 7.5 Hz, 12H). ^{13}C{^{1}H} NMR (100 MHz, DMSO-d_6) δ 156.62, 151.47, 141.99, 139.28, 138.55, 133.06, 132.24, 126.11, 46.52, 40.81, 38.72, 24.29, 14.65, 14.00. HRMS (APCI): calcd for $C_{35}H_{46}N_{10}O_6Na$ [M + Na]$^+$, 725.3494; found, 725.3473.

11. Synthesis of 1,1'-(hexane-1,6-diyl)bis(3-(2-(2-methyl-4-nitro-1H-imidazol-1-yl)ethyl)urea) (**4**): The precipitate was then washed with ethyl acetate to obtain the pure product as a white powder. Yield: 79.0%. ^{1}H NMR (400 MHz, DMSO-d_6) δ 8.21 (s, 2H), 5.94 (t, J = 5.8 Hz, 4H), 4.01 (t, J = 5.7 Hz, 4H), 3.37 – 3.29 (m, 4H), 2.92 (q, J = 6.5 Hz, 4H), 2.31 (s, 6H), 1.30 (m, 4H), 1.18 (m, 4H). ^{13}C{^{1}H} NMR (100 MHz, DMSO-d_6) δ 157.85, 145.34, 145.30, 122.27, 46.78, 39.50, 39.08, 29.88, 26.03, 12.45. HRMS (APCI): calcd for $C_{20}H_{32}N_{10}O_6Na$ [M + Na]$^+$, 531.2398; found, 531.2400.

12. Synthesis of 1,1'-(1,3-phenylenebis(propane-2,2-diyl))bis(3-(2-(2-methyl-4-nitro-1H-imidazol-1-yl)ethyl)urea) (**5**): The crude compound was purified by washing with diethyl ether and ethyl acetate. Yield: 79.0 %. ^{1}H NMR (400 MHz, DMSO-d_6) δ 8.20 (s, 2H), 7.27 (s, 1H), 7.22 – 7.09 (m, 1H), 7.11 – 6.89 (m, 2H), 6.28 (s, 2H), 5.91 (t, J = 6.0 Hz, 2H), 3.98 (t, J = 5.8 Hz, 4H), 3.34 – 3.27 (m, 4H), 2.32 (s, 6H), 1.47 (s, 12H). ^{13}C{^{1}H} NMR (100 MHz, DMSO-d_6) δ 156.84, 148.16, 145.33, 145.30, 127.22, 122.30, 122.23, 121.19, 54.23, 46.81, 39.08, 29.85, 12.52. HRMS (APCI): calcd for $C_{26}H_{36}N_{10}O_6Na$ [M + Na]$^+$, 607.2711; found, 607.2711.

13. Synthesis of 1,1'-(methylenebis(2,6-diethyl-4,1-phenylene))bis(3-(2-(2-methyl-4-nitro-1H-imidazol-1-yl)ethyl)urea) (**6**): Purification was performed by washing the crude compound with dichloromethane to yield a white powder. Yield: 80.0 %. ^{1}H NMR (400 MHz, DMSO-d_6) δ 8.18 (s, 2H), 7.39 (s, 2H), 6.92 (s, 4H), 6.26 (m, 2H), 4.04 (t, J = 5.8 Hz, 4H), 3.78 (s, 2H), 3.48 – 3.37 (m, 4H), 2.44 – 2.36 (m, 8H), 2.35 (s, 6H), 1.02 (t, J = 7.5 Hz, 12H). ^{13}C{^{1}H} NMR (100 MHz, DMSO-d_6) δ 157.07, 145.75, 145.68, 142.46, 139.50, 132.91, 126.63, 122.98, 47.35, 41.28, 24.76, 24.30, 15.05, 13.10. HRMS (APCI): calcd for $C_{35}H_{46}N_{10}O_6Na$ [M + Na]$^+$, 725.3494; found, 725.3459.

14. Synthesis of isometronidazole (2-(2-methyl-4-nitro-1H-imidazol-1-yl)ethan-1-ol) (**14**): A solution of 2-methyl-4-nitro-1H-imidazole (0.30 g, 2.4 mmol), potassium carbonate (0.97 g, 7.9 mmol), bromoethanol (830 µL, 11.8 mmol) and potassium iodide (0.39 g, 2.4 mmol) was added to DMF (20.0 mL) in a round bottomed flask and the mixture was stirred overnight at room temperature. The solvent was evaporated, dried and the mixture was purified by column chromatography in DCM using methanol gradient (0.0-0.5 %) and the product was recrystallized from ethanol/diethyl ether. Yield: 81.0 %. ^{1}H NMR (400 MHz, Methanol-d_4) δ 8.08 (s, 1H), 4.15 – 4.08 (m, 2H), 3.87 – 3.80 (m, 2H), 2.45 (s, 3H). ^{13}C{^{1}H} NMR (100 MHz, Methanol-d_4) δ 145.96, 145.48, 121.00, 60.32, 49.17, 11.48. HRMS (APCI): calcd for $C_6H_9N_3O_3Na$ [M + H]$^+$, 194.0536; found, 194.0537.

Gelation Details

Gelation Test. In a standard 7.0 mL vaial (ID =15.0 mm), an appropriate amount of the gelator and 1.0 mL of suitable solvent were added, and the vial was sealed. The mixture was then sonicated and heated until a clear solution was obtained. The solution was left undisturbed for gelation and a vial-inversion test was performed to confirm gelation.

Minimum Gel Concentration (MGC). The gel was prepared following the above procedure by dissolving the compounds in 1.0 mL of solvent. An additional amount of the solvent was added in portions, and the gelation process was repeated until a trace amount of the solvent was observed on the top of the gel. The excess solvent was removed, and MGC of the gelator was determined by calculating the weight percent of the compound.

T_{gel} Experiment. The appropriate amount of the gelator was taken in a standard 7.0 mL vial, and 1.0 mL of solvent was added. The mixture was sonicated and heated to dissolve and left undisturbed. A tiny spherical glass ball was carefully put on the top of the gel after 24 h and was heated in an oil bath fitted with a thermosensor and magnetic stirrer. The temperature of the oil bath was steadily raised by 10.0 °C per minute. The temperature at which the glass ball touched the bottom of the vial was recorded as T_{gel}.

Rheology: Rheological experiments were performed in nitrobenzene. The mechanical strength of the gelators was measured using MCR 102 Anton Paar modular compact rheometer with a 2.5 cm stainless steel parallel plate geometry. Gels were prepared by dissolving 30.0 mg of the corresponding gelator in 1.0 mL nitrobenzene. Experiments were carried out carefully by scoping a ~1.0 mL portion of gel on the plate. A Peltier temperature control hood was used to avoid the solvent evaporation and to maintain a temperature of 25.0 °C for frequency and amplitude sweeps. Amplitude sweeps were performed with a constant frequency of 1.0 Hz and log ramp strain (γ) = 0.01−100%, while the frequency sweeps were carried out between 0.1 and 10.0 Hz within the linear viscoelasticity domain (0.02% strain).

Scanning Electron Microscopy (SEM): The surface morphologies of the xerogels were examined using SEM. Gels of compounds (**1**-**6**) were prepared in nitrobenzene at 3.0 wt/v% and the gel was filtered after 24 hrs, dried in air to obtain the xerogel. A small portion of the xerogel was placed on a pin mount with the carbon tab on top, which was coated with gold for 5-6 min and was loaded on a Leo Supra 25 microscope at an operating voltage of 3.0 kV, and a working distance 3-4 mm. An in-lens detector was used to record the SEM images. We have also performed the SEM of dried gel of gelator **3** from DMSO/water (7:3, v/v, 3.0 wt/v%), ethanol (0.3 wt/v%) and 1,4-dioxane (0.5 wt/v%). The SEM of gelators **2** and **4** were performed on the xerogels from DMSO/water (1:1, v/v) at 5.0 wt/v%.

Crystallography

Single-crystal X-ray Diffraction: Single crystals of metronidazole and isometronidazole amine hydrochlorides were obtained by the slow evaporation of the acidic solution of the compounds in DMF/water (1:1 v/v) and ethanol/water (1:1 v/v), respectively. X-ray quality crystals of compound **2** were obtained by the slow evaporation of a nitromethane solution of the compound. X-ray analysis was performed on a Bruker D8 Venture (Photon100 CMOS detector) diffractometer equipped with a Cryostream (Oxford Cryosystems) open-flow nitrogen cryostats. The data for the crystals of metronidazole (**9.2HCl**) and isometronidazole (**12.HCl**) based amines were collected using CuK_α radiation (λ = 1.542 Å) at 295(2) K, and MoK_α radiation (λ = 0.71073 Å) at 150(2) K was used for gelator **2**. Apex-III software (Bruker AXS: Madison, WI, 2015) was used for the unit cell determination, data collection, data reduction, structure solution/refinement and empirical absorption correction. All structures were solved by direct method and refined by the full-matrix least squares on F^2 for all data using SHELXTL.[47] The disordered imidazole moieties and the solvent molecule of gelator **2** were modeled using free variable (FVAR) instructions and were refined isotropically. All other non-disordered non-hydrogen atoms were refined anisotropically. All the hydrogen atoms were placed in the calculated positions and refined using a riding model. Crystallographic data for the structures have been deposited to Cambridge Crystallographic Data Centre as supplementary publication (CCDC no: 2088742-2088744).

Powder X-ray Diffraction (PXRD): The PXRD of the isolated metronidazole crystals from gel phase crystallization and solution phase were recorded on a PANalytical instrument with 2θ ranging from 4.0−60.0⁰. The crystals were isolated from the crystallizing medium, washed with hexane, dried and ground to fine powder and PXRD was recorded. We have also performed the PXRD of the synthesized metronidazole and isometronidazole based amine hydrochlorides to ensure the purity of bulk products. Xerogels of **2** were prepared by filtering the gels from the corresponding solvents and the PXRD was performed after drying the xerogels in the fume hood for 16 hrs.

Gel phase crystallization: The gel phase crystallization was performed in nitrobenzene and aqueous solution (1:1, v/v) of DMSO and DMF. The experiments were performed in a standard 7.0 mL vial with the gelator and the drug molecule in 1.0 mL of the solvent. Experiments were performed at various concentrations of the gelator and the drug moiety to study the effect on the gel phase crystallization. The gels were removed after 24 h and analyzed under a Leica MC190 HD digital microscope. We have repeated several batches of gel phase crystallization experiments and the gels were analyzed at different time intervals (up to 3 weeks).

RESULTS AND DISCUSSION

~~We have designed gelators based on bis(urea) backbone with a complementary functional group similar to metronidazole and isometronidazole (Scheme 2). The urea motif chosen is well known to form α-tapes resulting in fibrils that could align the drug-derived functional groups as a locally ordered array on the surface of the gel fibers (Scheme 1).[3, 41, 42] The resulting LMWGs are anticipated to have a fibrous surface that chemically matches the crystallization substrate,[10] which offers the possibility of epitaxial crystal growth.[9]~~ Metronidazole and isometronidazole mimicking bis(urea) compounds (Scheme 2) were synthesized by reacting the corresponding amine precursors of these compounds with different diisocyanates (Scheme 3).

We have selected diisocyanates with different linkers, namely hexylene, sterically hindered *m*-dipropylenephenylene and tetraethyl diphenylmethane derivatives, which have been previously used as effective linkers for LMWGs.[10] The preparation of the amine precursors of metronidazole and isometronidazole is outlined in Scheme 3.
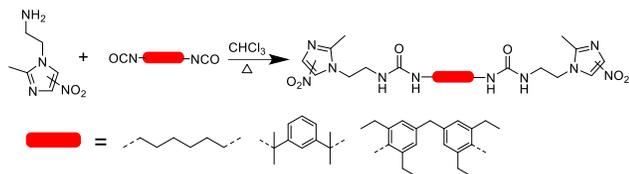
Scheme 23: Synthesis of metronidazole and isometronidazole bis(urea) compounds.

The hydroxyl group of metronidazole was converted to the bromo derivative *via* bromination, while the bromo derivative of isometronidazole was synthesized from 2-methyl-4(5)-nitroimidazole *via* substitution reaction with 1,2-diethyl bromide (Scheme S2, see supporting information).[10,48] The bromo derivatives were converted to azide and then reduced to the corresponding amines in presence of triphenylphosphine (Scheme 34). The products were then converted to the hydrochloride salts by treatment with dilute HCl.
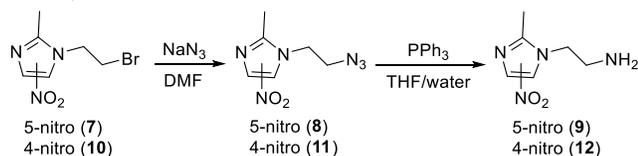
Scheme 34: Synthesis of metronidazole and isometronidazole based amine precursors.

The molecular structure of these two isomeric amine hydrochloride salts was confirmed by single-crystal X-ray diffraction (Table S1, S2 and Figure S13, see supporting information). The reaction of the metronidazole amine derivative in presence of Et₃N with the diisocyanates outlined in Scheme 2 in chloroform yielded compounds **1**, **2** and **3**, respectively. Similarly, the reaction of the isometronidazole amine derivative with these diisocyanates yielded **4**, **5** and **6**.
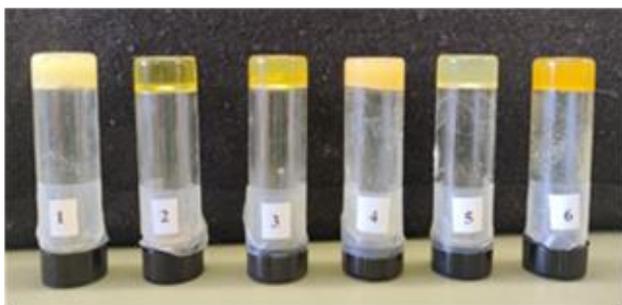
Figure 1: Gels of bis(urea) compounds (**1-6**) obtained from nitrobenzene.

Gelation studies: The gelation properties of the bis(urea) compounds were tested in a wide range of solvents (Table S3, see supporting information). The gelation tests were carried out by heating the gelator (10 mg) in a suitable solvent (1.0 mL) in a sealed vial (1.0 wt/v%) to give a transparent solution. The vial was left undisturbed, and the gel formation was confirmed by a vial inversion test. Metronidazole mimicking compounds (**1-3**) formed gels in nitrobenzene at 1.0 wt/v% (Figure 1) and gel formation was confirmed by a simple inversion test in all cases. Compound **2** formed gel in 1,2-dibromoethane, chlorobenzene and 1,4-dioxane at 2.0 wt/v%. The metronidazole mimicking diphenylmethane derivative (**3**) formed gel in cyclopentanone and cyclohexanone at 1.0 wt/v% and in ethylene glycol at 2.0 wt/v%. The insolubility of compound **3** at 1.0 wt/v% in alcohols and non-polar solvents prompted us to check the gelation properties at lower concentration (≤ 0.5 wt/v%) and gelation was

observed in ethanol, n-propanol, n-butanol, n-pentanol, 1,4-dioxane and nitromethane.

Table 1: Minimum gel concentration and T_{gel} at 3.0 wt/v% of the gelators in nitrobenzene.

Compound	MGC (wt/v%)	T_{gel} (°C)
1	0.8	103.7
2	0.9	84.3
3	0.5	151.4
4	2.8	145.4
5	2.5	118.8
6	2.8	153.8

The gelation studies of isometronidazole mimicking compounds (**4-6**) revealed that gelation was observed at higher concentration (3.0 wt/v%) in nitrobenzene compared to metronidazole derivatives **1–3**. In the case of compound **5**, sonication was required to induce gelation in nitrobenzene prior to cooling. The diphenylmethane derived isometronidazole analog (**6**) gelled ethylene glycol at 3.0 wt/v% and DMF at 4.0 wt/v%. We have also studied the gelation properties of these compounds in aqueous solution (1:1, v/v) of DMF and DMSO. Compound **6** formed gel in DMF/water at 3.0 wt/v% and compound **4** formed gels in DMSO/water and DMF/water at 4.0 and 5.0 wt/v%, respectively. Compound **3** formed gels in DMF/water and DMSO/water mixture at 3.0 wt/v% when the solvent combination was changed to 7:3 (v/v).

The minimum gel concentration (MGC) is the minimum amount of the compound required to form a self-supporting gel. The MGC of the gelators was evaluated in various solvents (Table S4, see supporting information). The MGC measurements of metronidazole-based gelators **1–3** in nitrobenzene (Table 1) establish that compound **3** has lower MGC values. Comparing the MGCs of mimetic and non-mimetic gels in nitrobenzene the MGCs of the non-mimetic compounds **4–6** are higher. Compound **3** can be considered as a supergelator in 1-propanol, ethanol, 1-butanol, nitromethane, 1,4-dioxane and 1-pentanol because the MGC is less than 0.5 wt/v% (Table S4, see supporting information). The MGC in DMSO/water for gelator **2** (1:1, v/v) and **3** (7:3, v/v) is 2.5 wt/v% and 3.0 wt/v%, respectively.

Thermal Stability: The thermal stability of the gels was evaluated by recording the transition temperature (T_{gel}) at which the gel converts to the solution phase. T_{gel} experiments were performed for all gels at 3.0 wt/v% in nitrobenzene and the results indicate that gelator **2** has the lowest T_{gel} value (Table 1). The T_{gel} experiments performed at lower concentration (1.0 wt/v%) for compounds **1–3** in nitrobenzene revealed the highest thermal stability for gels of **3** (Table S5, see supporting information), and the thermal stability increases with concentration. The thermal stability of the diphenylmethane derived gelator is higher than the other gelators in most cases (Table S5, see supporting information). The T_{gel} of the mimetic and the non-mimetic gelators in nitrobenzene were compared to see the effect of the spatial arrangement of the functional groups, which indicates that the thermal stability of the mimetic gels (**1–3**) is lower than non-mimetic gelators (**4–6**).

Mechanical strength: Rheology has been used to evaluate the solid-like properties and the stiffness of the gels.[49,50] Rheology is used to quantify the deformation and flow characteristics of supramolecular gels, and rheological experiments provide information about the gel structural characteristics.[51-53] The mechanical properties of the bis(urea) gelators were measured at

3.0 wt/v% in nitrobenzene. A strain sweep was performed to determine the linear viscoelastic region (LVR), at a constant frequency of 1.0 Hz, and the elastic modulus (G') was independent of the applied strain. Most of the gelators displayed a constant G' up to 0.1% strain, except for the compound **1**, where the G' value decreased after 0.02%. (Figure S14). The cross over point for gelators **2** and **5** were found to be around 0.5-3.0% strain, while the cross over point for gelators **1**, **3**, **4** and **6** is around 5.0–15.0% strain.
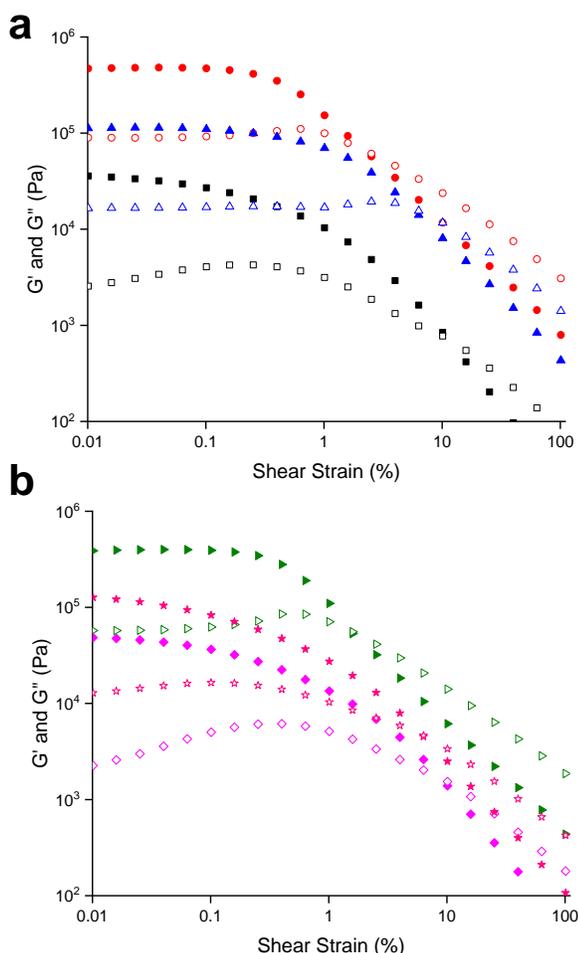
Figure 2: Amplitude sweep experiments of bis-(urea) gels (3.0 wt/v%) in nitrobenzene at 25.0 °C with a constant frequency of 1.0 Hz. Color codes: (a) gelator-**1** G' (■) and G'' (□), gelator-**2** G' (●) and G'' (○), gelator-**3** G' (▲) and G'' (△), and (b) gelator-**4** G' (◆) and G'' (◇), gelator-**5** G' (▶) and G'' (▷), gelator-**6** G' (★) and G'' (☆). Frequency sweep of bis(urea) gels (3.0 wt/v%) in nitrobenzene at 25.0 °C with a constant strain of 0.02%. Color codes: gelator-**1** G' (■) and G'' (□), gelator-**2** G' (●) and G'' (○), gelator-**3** G' (▲) and G'' (△), gelator-**4** G' (◆) and G'' (◇), gelator-**5** G' (▶) and G'' (▷), and gelator-**6** G' (★) and G''(☆).

Frequency sweep experiments were performed within a range of 0.1- 10 Hz at a constant strain of 0.02 %. A constant elastic (G') and viscous (G'') moduli under varying frequency establish that these materials are true gels (Figure 2). Interestingly, the mimetic gelator **2** displays higher G' and G'' compared to all the other gelators, indicating a comparatively stronger network in nitrobenzene. Gels of compounds **2** and **5** are stiffer (>200 kPa) compared to other bis(urea) gelators in nitrobenzene and the elastic modulus (G') is around twofold higher than the other

bis(urea) gels. Comparison of the mimetic gelators (**1**–**3**) revealed that gelator **2** displayed higher G' and G'' values indicating a strong gel network. The mechanical strength of the gel network in **3** was more robust than gelator **1**. For the non-mimetic gelators (**4**–**6**), the gel of **5** was found to be a stiffer gel, and the G' and G'' values of gels of **4** and **6** were comparable and low, suggesting a weaker gel-network in these gels. The difference in mechanical strength for **2** and **5** may be attributed to the favorable network formation in nitrobenzene compared to others.
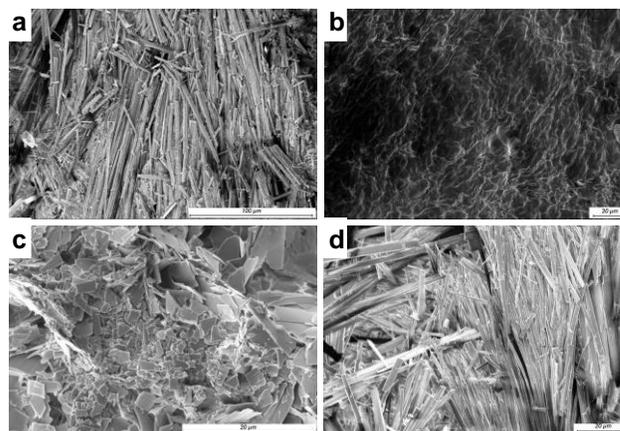
Figure 3: SEM images of the xerogel of (a) **1** (b) **2** (c) **4** and (d) **6** from nitrobenzene at 3.0 wt/v%.

Gel Morphology: The morphology of the dried gel fibrils was analyzed by scanning electron microscopy (SEM). SEM performed on the dried gels of all the gelators from nitrobenzene (3.0 wt/v%) revealed a fibrous network in most cases. Gelator **1** displayed needle-shaped morphology (Figure 3a) with a thickness ranging from 1.0-3.0 µm. Gelator **2**, **3** and **5** displayed an entangled fibrous network (Figure 3b & Figure S15-16, see supporting information) and the diameter of the fibers ranged from 200-400 nm. The gelator **4** displayed a plate-shaped morphology with a diameter of around 1.0-4.0 µm (Figure 3c). The dibenzyl linker-based gelator **6** displayed long needle-shaped morphology (Figure 3d).
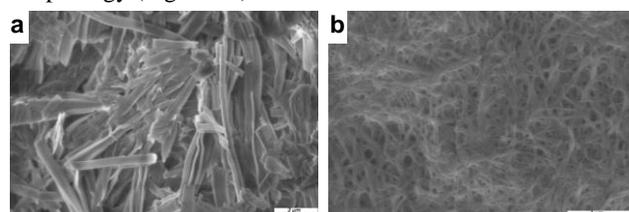
Figure 4: SEM images of gelator **3**: from (a) DMSO/water (7:3, v/v) at 3.0 wt/v% and (b) 1-4 dioxane (0.5 wt/v%).

SEM images recorded for gelator **3** at 3.0 wt/v% in DMSO/water (7:3, v/v) displayed needle-shaped morphology (Figure 4a).[54-56] Similarly, the SEM images of gelator **4** from DMSO/water (1:1, v/v) at 4.0 wt/v% displayed thicker needles (Figure S17, see supporting information). We have also performed the SEM of gelator **3** xerogel obtained from 1,4-dioxane (0.5 wt/v%, Figure 4b) and ethanol (0.33 wt/v%, Figure S18, see supporting information) and the images displayed helical fibrous aggregates with fiber thickness ranging from 20-40 nm.

Single crystal X-ray diffraction: X-ray quality single crystals of **2** were obtained *via* slow cooling of the nitromethane solution and characterized by X-ray crystallography (Figure S19 and Table S4 and S5, see supporting information). The com-

pound displays the characteristic one-dimensional (1-D) hydrogen bonded urea α-tape motif resulting from the complementary crisscross urea hydrogen bonding from one of the urea moieties (Figure 5a). These 1-D zig-zag tapes interact with adjacent tapes *via* N-H···O hydrogen bonding interaction arising from the second urea motif to form a 2-D hydrogen bonded sheet architecture Figure 5b). The nitrogen and oxygen atoms of the imidazole moiety of adjacent 2-D networks interact each other to form voids with entrapped nitromethane (Figure S19, see supporting information). The comparison of the powder X-ray diffraction pattern (PXRD) of the bulk crystal with the simulated pattern obtained from the crystal structure[21, 56-58] confirmed the phase purity of the crystals (Figure S20, see supporting information). The comparison of the powder diffraction pattern of either the native gel or the dried gel with the calculated pattern from the crystal structure can provide information about the structure of xerogels.[21, 56-59] Although, the drying process can result in artefacts,[60] this approach may provide useful information about the self-assembly process in LMWGs.[1, 7, 21, 56-59] The comparison of the PXRD pattern of the dried gel from nitrobenzene with the crystal structure indicated that the two materials are different solid forms. However, the PXRD pattern of the xerogel of **2** from nitrobenzene and chlorobenzene matched with the pattern of bulk crystals of a second solid form of **2** obtained from isopropanol. The PXRD pattern of the DMSO/water (1:1, v/v) xerogels proved to be more similar to the pattern calculated from the single crystal structure (Figure S21, see supporting information). These results indicate that there are at least two types of the gelator structure obtained depending on the crystallising or gelling solvent.
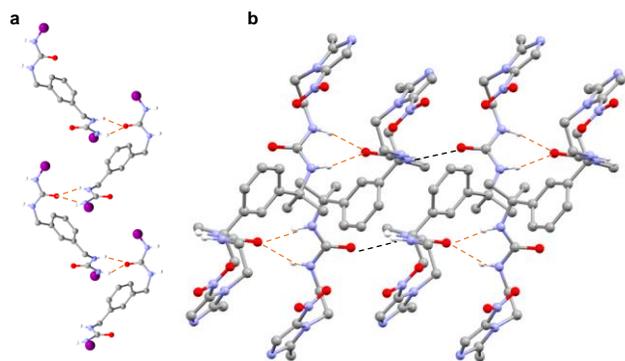
Figure 5: Illustration of crystal structure in **2** (a) 1- D hydrogen bonded zig-zag chains via complementary urea hydrogen bonding (The purple sphere represents the metronidazole mimetic fragment) and (b) adjacent 1-D chains interact with each other (broken black lines) to form a 2-D hydrogen bonded network.

Gel phase crystallization: The ability of the gelators to gel nitrobenzene prompted us to select nitrobenzene as a solvent for gel phase crystallization of the target drug material. The metronidazole was purified by recrystallization from DMSO/water (1:1, v/v) prior to crystallization studies. Initially we performed the solution phase crystallization of metronidazole from nitrobenzene to optimize the crystallization conditions. This gave plate-shaped crystals of metronidazole in a herringbone fashion (Figure 6a) was observed in nitrobenzene (30 mg/mL) after a day (Table S6, see supporting information). Experiments performed at higher concentrations also resulted in crystals with similar morphology after 2-3 hrs.

Gel phase crystallization was performed by dissolving metronidazole and the gelators in 1.0 mL nitrobenzene, and the

mixture was sonicated and heated to yield a transparent solution. The solution was left undisturbed at ambient temperature, and gelation was observed in 5-10 minutes. The gels were analyzed by polarized light microscopy after 24 hours, which indicated the formation of crystals within the gels in most cases (Table S7, see supporting information). The optimized concentration of metronidazole was found to be 50 mg/mL and the experiments performed with 30 mg/mL did not result in any crystals after 2-3 weeks. The experiments were performed at 2.0 wt/v% for gelator **1** because the gels were not stable at lower concentrations in the presence of crystallization substrate. Analysis of the crystals obtained from gelator **1** indicated that needle-shaped crystals were formed (Figure 6b). The experiments performed in gelators **2** at 1.0 wt/v% yielded transparent gels and crystal growth was observed after 24 hours (Figure S22, see supporting information). The morphology of the crystals was found to be similar to the crystals from gelator **1** (Figure 6c).
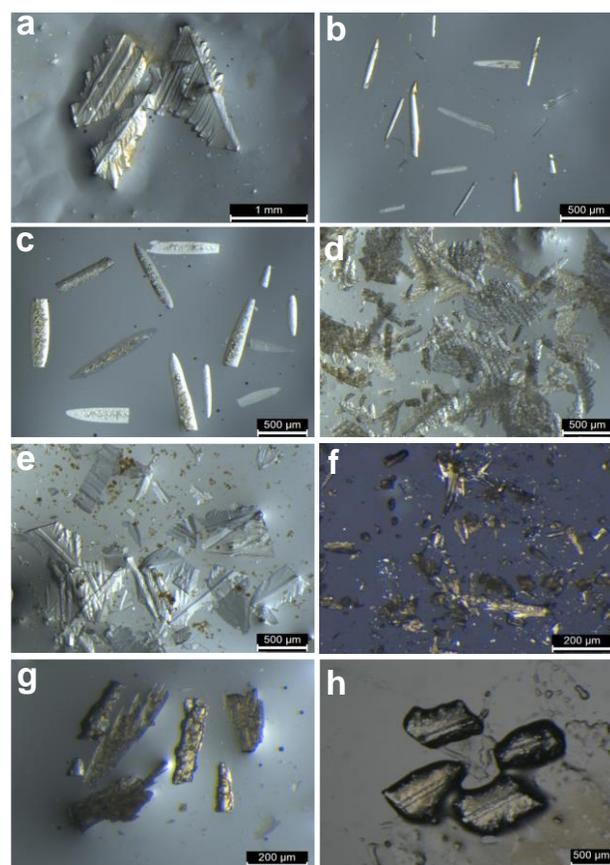
Figure 6. Comparison of crystals of metronidazole from solution and gel phase crystallization (GPC) in nitrobenzene. (a) Solution phase and (b) gel phase crystallization in **1**, (c) **2**, (d) **3**, (e) **4**, (f) **5**, (g) **6** and (h) alanine gelator, respectively.

Gel phase crystallization in gelator **3** at 1.0 wt/v% resulted in a herringbone pattern of needle-shaped crystals clumped together (Figure 6d). Gel phase crystallization experiments were performed in several batches, and the crystals were analyzed at different time intervals over 2–3 weeks, which indicated that the morphologies of the crystals were consistent batch-to-batch and over time. The crystallization experiments were repeated with increasing concentration of metronidazole (75 and 100 mg/mL) and the morphologies were similar to the 50 mg/mL experiments. The experiments performed at 3.0 wt/v% of the gelators **1**–**3** also resulted in morphologies similar to 1.0 wt/v% of the corresponding gelators.

For comparison gel phase crystallization was also carried out with the non-metronidazole-mimetic gelators **4**–**6**. A gelator concentration of 6.0 wt/v% (Table S8, see supporting information) was used to avoid dissolution of gels in the presence of crystallization substrate. The experimental procedure was similar to the mimetic gels and partial gels was observed for gelator **5** in the presence of metronidazole. Plate shaped crystals in a herringbone morphology were observed for gels of gelator **4**, and similar results were observed at higher concentration of metronidazole (Figure 6e). Gel phase crystallization experiments in gelator **5** was achieved by sonicating the mixture prior to cooling, but crystals were not formed even at higher concentration of metronidazole after a month. Analysis of the partial gels of gelator **5** obtained by normal gel phase crystallization procedure indicated the formation of micro-needle crystals of metronidazole (Figure 6f). The experiments performed with gelator **6** resulted in clusters of crystals arranged in a herringbone fashion (Figure 6g). Crystallization of metronidazole was also undertaken in an unrelated (non-metronidazole-mimetic) bis(urea) gelator based on L-phenyl alanine methyl ester at 2.0 wt/v% (Figure S23, see supporting information) which resulted in plate shaped crystals clumped in a herringbone pattern (Figure 6h). The needle shape morphology obtained in the case of the mimetic gels may be attributed to the epitaxial growth of metronidazole crystals on gel fibers due to their favorable interactions with structurally similar functional groups of the LMWGs.
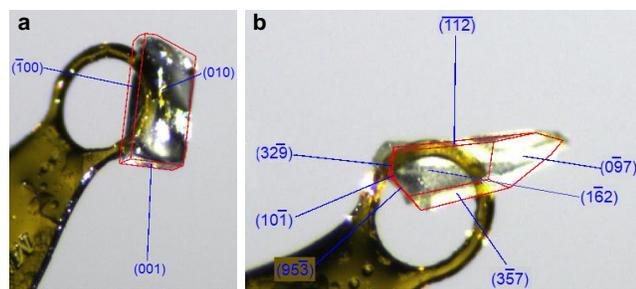
Figure 7: Face-indexed morphology of metronidazole crystals (a) grown from nitrobenzene solution, (b) wedge-shaped crystal from a nitrobenzene gel of metronidazole-mimetic gelator **3** expressing higher order faces.

Face indexing of representative crystals grown from solution and from gels of compounds **1** – **6** revealed complex and varied influence of all the gels on morphology. The solution grown crystals have a relatively simple morphology and express faces with mainly low indices, namely ($\bar{1}00$), ($0\bar{1}0$) and ($00\bar{1}$) as well as a large ($1\bar{1}\bar{5}$) face, the morphology of gel-grown crystals proved much more complex and unique to each gel with multiple high-index faces being expressed. For example, crystals obtained from nitrobenzene gels of **3** exhibit a wedge shape expressing a large ($0\bar{9}7$) face, Figure 7. Other gel-grown samples all expressed a wide variety of faces and asymmetric morphology (supplementary information Figures S27–S33, see supporting information). This implies a variety of specific adsorption modes of the gel fibers to the growing crystals.

We have performed the rheology experiments of the gels in the presence of metronidazole (50 mg/mL) in nitrobenzene at 3.0 wt/v%, and isometronidazole mimicking gels formed partial gels. The mechanical strength of the mimetic gels (**1-3**) was increased in the presence of the drug additive (Figure S34 & S35, see supporting information). At higher gelator concentration (6.0 wt/v%) gels were observed in all cases with increased mechanical strength compared to the corresponding gels without drug additives, expect for **4** and **5** (Figure S36S35 S39S36, see supporting information). This prompted us to check whether the discrepancy in the stabilities is related to the kinetic trapping of the self-assembled structures by annealing the gels.[61, 62] This was achieved by performing a gel-to-sol transition by heating the gels after 12 hours and the solution thus obtained was left undisturbed for gelation. The mechanical strength of mimetic and non-mimetic gels did not show any drastic change compared to the corresponding non-annealed gels (Figure S37-40, see supporting information). The mechanical strength of the mimetic gels (**1-5**) in the presence of the metronidazole displayed similar results compared to the corresponding non-annealed gels but the mechanical strength of **6** decreased after annealing (Figure S38-39, see supporting information). However, the thermal stabilities of the gels were found to be lower in the presence of the additives (Table S9 S11S10). The enhanced mechanical properties of the mimicking gelators (**1-3**) in the presence of crystallization substrate indicate a favorable interaction of the gelator molecules with the substrates presumably due to the similarity in the functional group. However, a reverse phenomenon was observed for the non-mimetic gelators (**4-6**), which clearly indicate the importance of structural similar functional groups in LMWGs and the crystallization substrates.

In contrast to nitrobenzene, solution phase crystallization of metronidazole in aqueous DMF and DMSO (1:1 and 7:3, v/v) resulted in long needle-shaped crystals (Figure S24, see supporting information). The gel phase crystallization with gelator **2** in DMSO/water (1:1, v/v) resulted in needle-shaped crystals, while micro-needle shaped crystals were obtained with gelator **3** in DMSO/water (7:3, v/v) and gelator **4** in DMSO/water (1:1, v/v, (Figure S25, see supporting information). The gel phase crystallization in DMF/water (1:1, v/v) with gelator **4** and **6** resulted in micro-needle crystals, respectively. Thus, unlike nitrobenzene, gel phase crystallization in aqueous DMF and DMSO does not show crystal habit modification with any gelator, presumably due to the interaction of LMWGs with hydrogen bonding solvents, which prevents the drug from interacting with the complimentary sites in the gelators.

The role of LMWGs in tuning crystallization was analyzed by performing solution phase crystallization in the presence of dissolved gelators **3**, **4**, **5** and **6**, which resulted in plate-shaped crystals clumped in a herringbone pattern similar to the solution phase crystal morphology (Figure S26, see supporting information). However, the experiments with **1** and **2** displayed a mixture of plate-shaped crystals with herringbone patterns and needle-shaped crystals. These results suggest that the gel medium plays a vital role in inducing crystal habit modification rather than just the gelator molecule itself in solution. The solution/gel phase crystallization of isometronidazole did not yield any crystals.
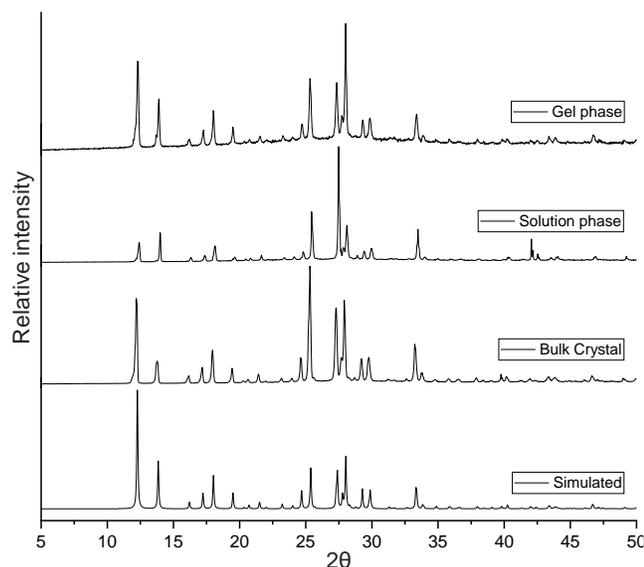
Figure 8: Comparison of PXRD pattern of metronidazole: simulated from single crystal data, bulk crystals obtained from DMSO/water, crystals from solution phase and gel phase crystallization from gelator **1** in nitrobenzene.

X-ray analysis performed on all the crystals revealed no difference in polymorphic form with the known form-I[36] produced in all cases. The phase purity of the bulk crystal was analyzed by comparing the PXRD of the bulk crystal with the simulated pattern obtained from the crystal structure reported.[21, 56-58] This data was obtained using bulk crystals isolated from the gel phase and solution phase crystallization experiments. The comparison of the PXRD pattern of the metronidazole crystals from the solution and gel phase crystallization with the simulated pattern of the crystal structure revealed super-imposable patterns (Figure 8 & Figure S4~~0~~1, see supporting information), indicating phase purity of the bulk solid.

CONCLUSIONS

We have synthesized six bis(urea) compounds with functional groups mimicking either metronidazole (**1-3**) or its isomer isometronidazole (**4**–**6**). The gelation studies revealed that metronidazole-mimetic compound **3** gels various solvents compared to the isomeric gelator **6**. The T_{gel} experiments suggested that gels based on the isometronidazole gelators **4**–**6** have higher thermal stability than the mimetic gels **1**–**3**. The comparison of the mechanical strength of the gelators in nitrobenzene revealed that the metronidazole-mimetic gelators **2** and **3** are more mechanically robust compared to the isomeric analogues **5** and **6**, but the hexylene-linker based gelator **4** forms a stronger gel compared with that of gelator **1**. The morphologies of the gelators were analyzed by SEM, which showed the presence of the entangled networks in most cases. Gel phase crystallization was performed in nitrobenzene since all the compounds formed gels in this solvent. The morphology of metronidazole crystals obtained from solution phase and gel phase crystallization were analyzed by polarized light microscopy. Plate-shaped crystals aggregated in a herringbone fashion were observed from solution phase crystallization. Crystallization from the isometronidazole based gels displayed different morphologies such as plate-shaped (**4**), microcrystals (**5**), and thicker needles (**6**). The morphologies of the crystals obtained from the mimetic metronidazole gel (**1-3**) were consistent, displaying needle-shaped

crystals, and the needle-shaped crystals in **3** were clumped together in a herringbone fashion. The results indicate that crystal habit modification (plate to needle morphology) arises selectively from gels based on the mimetic gelators. This crystal habit modification can be attributed to adsorption of the growing crystals on to the surface of the gel fibers and potentially epitaxial crystal growth in the case of the mimetic gels.

ASSOCIATED CONTENT

Supporting Information
^{1}H NMR spectra, further gelation studies, rheology, SEM images, single crystal X-ray diffraction and PXRD of metronidazole/iso-metronidazole mimetic amines and gelator **2**, face indexing and comparison of PXRD metronidazole from different gelators are provided as Supporting Information. This material is available free of charge via the Internet at http://pubs.acs.org.

AUTHOR INFORMATION

Corresponding Author

Krishna K. Damodaran, E-mail: krishna@hi.is.
Jonathan W. Steed, E-mail: jon.steed@durham.ac.uk

Notes
The authors declare no competing financial interests.

ACKNOWLEDGMENT

REFERENCES

(1)   Dastidar, P., Supramolecular gelling agents: can they be designed? *Chem. Soc. Rev.* **2008,** 37, (12), 2699-2715.
(2)   de Loos, M.; Feringa, B. L.; van Esch, J. H., Design and Application of Self-Assembled Low Molecular Weight Hydrogels. *Eur. J. Org. Chem.* **2005,** 2005, (17), 3615-3631.
(3)   Estroff, L. A.; Hamilton, A. D., Water Gelation by Small Organic Molecules. *Chem. Rev.* **2004,** 104, (3), 1201-1218.
(4)   George, M.; Weiss, R. G., Molecular Organogels. Soft Matter Comprised of Low-Molecular-Mass Organic Gelators and Organic Liquids†. *Acc. Chem. Res.* **2006,** 39, (8), 489-497.
(5)   Hirst, A. R.; Escuder, B.; Miravet, J. F.; Smith, D. K., High-Tech Applications of Self-Assembling Supramolecular Nanostructured Gel-Phase Materials: From Regenerative Medicine to Electronic Devices. *Angew. Chem. Int. Ed.* **2008,** 47, (42), 8002-8018.
(6)   Steed, J. W., Anion-tuned supramolecular gels: a natural evolution from urea supramolecular chemistry. *Chem. Soc. Rev.* **2010,** 39, (10), 3686-3699.
(7)   Yu, G.; Yan, X.; Han, C.; Huang, F., Characterization of supramolecular gels. *Chem. Soc. Rev.* **2013,** 42, (16), 6697-6722.
(8)   Liesegang, R. E., Chemische Reaktionen in Gallerten. *Naturwiss. Wochenschr.* **1896,** 11, 353.
(9)   Kumar, D. K.; Steed, J. W., Supramolecular gel phase crystallization: orthogonal self-assembly under non-equilibrium conditions. *Chem. Soc. Rev.* **2014,** 43, (7), 2080-2088.
(10) Foster, J. A.; Damodaran, K. K.; Maurin, A.; Day, G. M.; Thompson, H. P. G.; Cameron, G. J.; Bernal, J. C.; Steed, J. W.,

Pharmaceutical polymorph control in a drug-mimetic supramolecular gel. *Chem. Sci.* **2017,** 8, (1), 78-84.

(11) Hektisch, H. K.; Dennis, J.; Hanoka, J. I., Crystal growth in gels. *J. Phys. Chem. Solids* **1965,** 26, (3), 493-496.

(12) Duffus, C.; Camp, P. J.; Alexander, A. J., Spatial Control of Crystal Nucleation in Agarose Gel. *J. Am. Chem. Soc.* **2009,** 131, (33), 11676-11677.

(13) Buerkle, L. E.; Rowan, S. J., Supramolecular gels formed from multi-component low molecular weight species. *Chem. Soc. Rev.* **2012,** 41, (18), 6089-6102.

(14) Edwards, W.; Smith, D. K., Enantioselective Component Selection in Multicomponent Supramolecular Gels. *J. Am. Chem. Soc.* **2014,** 136, (3), 1116-1124.

(15) Cross, E. R.; Sproules, S.; Schweins, R.; Draper, E. R.; Adams, D. J., Controlled Tuning of the Properties in Optoelectronic Self-Sorted Gels. *J. Am. Chem. Soc.* **2018,** 140, (28), 8667-8670.

(16) Draper, E. R.; Eden, E. G. B.; McDonald, T. O.; Adams, D. J., Spatially resolved multicomponent gels. *Nat. Chem.* **2015,** 7, 848.

(17) Colquhoun, C.; Draper, E. R.; Eden, E. G. B.; Cattoz, B. N.; Morris, K. L.; Chen, L.; McDonald, T. O.; Terry, A. E.; Griffiths, P. C.; Serpell, L. C.; Adams, D. J., The effect of self-sorting and co-assembly on the mechanical properties of low molecular weight hydrogels. *Nanoscale* **2014,** 6, (22), 13719-13725.

(18) Raeburn, J.; Adams, D. J., Multicomponent low molecular weight gelators. *Chem. Commun.* **2015,** 51, (25), 5170-5180.

(19) Estroff, L. A.; Addadi, L.; Weiner, S.; Hamilton, A. D., An organic hydrogel as a matrix for the growth of calcite crystals. *Org. Biomol. Chem.* **2004,** 2, (1), 137-141.

(20) Aparicio, F.; Matesanz, E.; Sanchez, L., Cooperative self-assembly of linear organogelators. Amplification of chirality and crystal growth of pharmaceutical ingredients. *Chem. Commun.* **2012,** 48, (46), 5757-5759.

(21) Ghosh, D.; Ferfolja, K.; Drabavičius, Ž.; Steed, J. W.; Damodaran, K. K., Crystal habit modification of Cu(ii) isonicotinate–N-oxide complexes using gel phase crystallisation. *New J. Chem.* **2018,** 42, (24), 19963-19970.

(22) Kennedy, S. R.; Jones, C. D.; Yufit, D. S.; Nicholson, C. E.; Cooper, S. J.; Steed, J. W., Tailored supramolecular gel and microemulsion crystallization strategies - is isoniazid really monomorphic? *CrystEngComm* **2018,** 20, (10), 1390-1398.

(23) Foster, J. A.; Piepenbrock, M.-O. M.; Lloyd, G. O.; Clarke, N.; Howard, J. A. K.; Steed, J. W., Anion-switchable supramolecular gels for controlling pharmaceutical crystal growth. *Nat. Chem.* **2010,** 2, 1037.

(24) Diao, Y.; Whaley, K. E.; Helgeson, M. E.; Woldeyes, M. A.; Doyle, P. S.; Myerson, A. S.; Hatton, T. A.; Trout, B. L., Gel-Induced Selective Crystallization of Polymorphs. *J. Am. Chem. Soc.* **2012,** 134, (1), 673-684.

(25) Pauchet, M.; Morelli, T.; Coste, S.; Malandain, J.-J.; Coquerel, G., Crystallization of (±)-Modafinil in Gel: Access to Form I, Form III, and Twins. *Cryst. Growth Des.* **2006,** 6, (8), 1881-1889.

(26) Kaufmann, L.; Kennedy, S. R.; Jones, C. D.; Steed, J. W., Cavity-containing supramolecular gels as a crystallization tool for hydrophobic pharmaceuticals. *Chem. Commun.* **2016,** 52, (66), 10113-10116.

(27) Daly, R.; Kotova, O.; Boese, M.; Gunnlaugsson, T.; Boland, J. J., Chemical Nano-Gardens: Growth of Salt Nanowires from Supramolecular Self-Assembly Gels. *ACS Nano* **2013,** 7, (6), 4838-4845.

(28) Kennedy, S. R.; Jones, C. D.; Yufit, D. S.; Nicholson, C. E.; Cooper, S. J.; Steed, J. W., Tailored supramolecular gel and microemulsion crystallization strategies – is isoniazid really monomorphic? *CrystEngComm* **2018,** 20, (10), 1390-1398.

(29) Dawn, A.; Andrew, K. S.; Yufit, D. S.; Hong, Y.; Reddy, J. P.; Jones, C. D.; Aguilar, J. A.; Steed, J. W., Supramolecular Gel Control of Cisplatin Crystallization: Identification of a New Solvate Form Using a Cisplatin-Mimetic Gelator. *Cryst. Growth Des.* **2015,** 15, (9), 4591-4599.

(30) Saikia, B.; Mulvee, M. T.; Torres-Moya, I.; Sarma, B.; Steed, J. W., Drug Mimetic Organogelators for the Control of

(31) Shinn, D., Metronidazole in acute ulcerative gingivitis. *The Lancet* **1962,** 279, (7240), 1191.

(32) Tally, F. P.; Sutter, V. L.; Finegold, S. M., Metronidazole versus anaerobes. In vitro data and initial clinical observations. *Calif. Med.* **1972,** 117, (6), 22-6.

(33) Tally, F. P.; Sutter, V. L.; Finegold, S. M., Treatment of anaerobic infections with metronidazole. *Antimicrob. Agents Chemother.* **1975,** 7, (5), 672-5.

(34) Löfmark, S.; Edlund, C.; Nord, C., Metronidazole Is Still the Drug of Choice for Treatment of Anaerobic Infections. *Clin. Infect. Dis.* **2010,** 50 Suppl 1, S16-23.

(35) Groom, C. R.; Bruno, I. J.; Lightfoot, M. P.; Ward, S. C., The Cambridge Structural Database. *Acta Crystallogr. Sect. B* **2016,** 72, (2), 171-179.

(36) Blaton, N. M.; Peeters, O. M.; De Ranter, C. J., 2-(2-Methyl-5-nitro-1-imidazolyl)ethanol (metronidazole). *Acta Crystallogr. Sect. B* **1979,** 35, (10), 2465-2467.

(37) Di Martino, P.; Censi, R.; Malaj, L.; Capsoni, D.; Massarotti, V.; Martelli, S., Influence of solvent and crystallization method on the crystal habit of metronidazole. *Cryst. Res. Technol.* **2007,** 42, (8), 800-806.

(38) Bhattacharjee, S.; Bhattacharya, S., Role of synergistic [small pi]-[small pi] stacking and X-H[three dots, centered]Cl (X = C, N, O) H-bonding interactions in gelation and gel phase crystallization. *Chem. Commun.* **2015,** 51, (32), 7019-7022.

(39) Jones, C. D.; Steed, J. W., Gels with sense: supramolecular materials that respond to heat, light and sound. *Chem. Soc. Rev.* **2016,** 45, (23), 6546-6596.

(40) Dawn, A.; Mirzamani, M.; Jones, C. D.; Yufit, D. S.; Qian, S.; Steed, J. W.; Kumari, H., Investigating the effect of supramolecular gel phase crystallization on gel nucleation. *Soft Matter* **2018,** 14, (46), 9489-9497.

(41) van Esch, J.; Kellogg, R. M.; Feringa, B. L., Di-urea compounds as gelators for organic solvents. *Tetrahedron Lett.* **1997,** 38, (2), 281-284.

(42) Schoonbeek, F. S.; van Esch, J. H.; Hulst, R.; Kellogg, R. M.; Feringa, B. L., Geminal Bis-ureas as Gelators for Organic Solvents: Gelation Properties and Structural Studies in Solution and in the Gel State. *Chem. Eur. J.* **2000,** 6, (14), 2633-2643.

(43) Romero, M. A., Synthesis of New Energetic Materials and Ionic Liquids Derived from Metronidazole. *Org. Chem. Int.* **2016,** 2016, 1-8.

(44) Wu, M.; El-Kattan, Y.; Lin, T.-H.; Ghosh, A.; Vadlakonda, S.; Kotian, P. L.; Babu, Y. S.; Chand, P., Synthesis of 9-[1-(Substituted)-3-(phosphonomethoxy)propyl]adenine Derivatives as Possible Antiviral Agents. *Nucleosides Nucleotides Nucleic Acids* **2005,** 24, (10-12), 1543-1568.

(45) Xu, Z.; Zhang, S.; Feng, L.-S.; Li, X.-N.; Huang, G.-C.; Chai, Y.; Lv, Z.-S.; Guo, H.-Y.; Liu, M.-L., Synthesis and In Vitro Antimycobacterial and Antibacterial Activity of 8-OMe Ciprofloxacin-Hydrozone/Azole Hybrids. *Molecules* **2017,** 22, (7), 1171.

(46) Akae, Y.; Iijima, K.; Tanaka, M.; Tarao, T.; Takata, T., Main Chain-Type Polyrotaxanes Derived from Cyclodextrin-Based Pseudo[3]rotaxane Diamine and Macromolecular Diisocyanate: Synthesis, Modification, and Characterization. *Macromolecules* **2020,** 53, (6), 2169-2176.

(47) Sheldrick, G. M., Crystal structure refinement with SHELXL. *Acta Crystallogr. Sect. C: Cryst. Struct. Chem.* **2015,** 71, (Pt 1), 3-8.

(48) Kajfez, F.; Sunjic, V.; Kolbah, D.; Fajdiga, T.; Oklobdzija, M., 1-Substitution in 2-methyl-4(5)-nitroimidazole. I. Synthesis of compounds with potential antitrichomonal activity. *J. Med. Chem.* **1968,** 11, (1), 169-171.

(49) Chapter 1 Introduction. In *Rheology for Chemists: An Introduction (2)*, The Royal Society of Chemistry: 2008; pp 1-13.

(50) Guenet, J.-M., *Organogels: Thermodynamics, structure, solvent role, and properties*. ed.; Springer: 2016.

(51) Dawn, A.; Kumari, H., Low Molecular Weight Supramolecular Gels Under Shear: Rheology as the Tool for Elucidating

Structure–Function Correlation. *Chem. Eur. J.* **2018,** 24, (4), 762-776.

(52) Sathaye, S.; Mbi, A.; Sonmez, C.; Chen, Y.; Blair, D. L.; Schneider, J. P.; Pochan, D. J., Rheology of peptide- and protein-based physical hydrogels: Are everyday measurements just scratching the surface? *Wiley Interdiscip. Rev. Nanomed. Nanobiotechnol.* **2015,** 7, (1), 34-68.

(53) Draper, E. R.; Adams, D. J., Low-Molecular-Weight Gels: The State of the Art. *Chem* **2017,** 3, (3), 390-410.

(54) Jin, Q.; Zhang, L.; Liu, M., Solvent-Polarity-Tuned Morphology and Inversion of Supramolecular Chirality in a Self-Assembled Pyridylpyrazole-Linked Glutamide Derivative: Nanofibers, Nanotwists, Nanotubes, and Microtubes. *Chem. Eur. J.* **2013,** 19, (28), 9234-9241.

(55) Tómasson, D. A.; Ghosh, D.; Kržišnik, Z.; Fasolin, L. H.; Vicente, A. A.; Martin, A. D.; Thordarson, P.; Damodaran, K. K., Enhanced Mechanical and Thermal Strength in Mixed-Enantiomers-Based Supramolecular Gel. *Langmuir* **2018,** 34, (43), 12957-12967.

(56) Ghosh, D.; Farahani, A. D.; Martin, A. D.; Thordarson, P.; Damodaran, K. K., Unraveling the Self-Assembly Modes in Multicomponent Supramolecular Gels Using Single-Crystal X-ray Diffraction. *Chem. Mater.* **2020,** 32, (8), 3517-3527.

(57) Ghosh, D.; Lebedytė, I.; Yufit, D. S.; Damodaran, K. K.; Steed, J. W., Selective gelation of N-(4-pyridyl)nicotinamide by copper(ii) salts. *CrystEngComm* **2015,** 17, (42), 8130-8138.

(58) Ghosh, D.; Bjornsson, R.; Damodaran, K. K., Role of N–Oxide Moieties in Tuning Supramolecular Gel-State Properties. *Gels* **2020,** 6, (4), 41.

(59) Tómasson, D. A.; Ghosh, D.; Kurup, M. R. P.; Mulvee, M. T.; Damodaran, K. K., Evaluating the role of a urea-like motif in enhancing the thermal and mechanical strength of supramolecular gels. *CrystEngComm* **2021,** 23, (3), 617-628.

(60) Adams, D. J., Does Drying Affect Gel Networks? *Gels* **2018,** 4, (2), 32.

(61) Fuentes-Caparrós, A. M.; de Paula Gómez-Franco, F.; Dietrich, B.; Wilson, C.; Brasnett, C.; Seddon, A.; Adams, D. J., Annealing multicomponent supramolecular gels. *Nanoscale* **2019,** 11, (7), 3275-3280.

(62) Panja, S.; Fuentes-Caparrós, A. M.; Cross, E. R.; Cavalcanti, L.; Adams, D. J., Annealing Supramolecular Gels by a Reaction Relay. *Chem. Mater.* **2020,** 32, (12), 5264-5271.

For Table of Contents Only